Effects of Infiltration on Chemical Transport into Overland Flow

J. K. Snyder, D. A. Woolhiser
MEMBER
ASAE

This article is reprinted from the TRANSACTIONS of the ASAE (Vol. 28, No. 5, pp. 1450–1457, 1985)
Published by the American Society of Agricultural Engineers, St. Joseph, Michigan

ABSTRACT

THE effect of raindrop impact and infiltration on the mixing process between surface runoff and tracer dye in a saturated porous medium (Ottawa sand) was studied in the laboratory. Experiments were conducted in a tilting plexiglass flume 10 cm wide, 200 cm long, and 30 cm deep. Infiltration and rainfall rate and energy could be closely controlled, and the mixing process at the surface was easily observed. Samples of pore fluid were obtained by withdrawing fluid through rubber septa with a microsyringe, and concentrations were measured by fluorometry. A complete description of the apparatus is presented, along with the results of 21 simulated rainstorm events. The mass of dye removed in overland flow was positively related to slope of the flume and negatively related to infiltration rate. The solute concentration profiles in the porous media, with zero slope and no infiltration, were convex upward. With infiltration, the profiles assumed a characteristic "s" shape. These observations suggest that the complete mixing model may be appropriate when infiltration rates are high, but an incomplete mixing model, or a convective dispersion model, would provide better approximations at low infiltration rates. Unexpected patterns of infiltration and exfiltration were observed at the surface of the porous medium when the flume was tilted. These patterns were probably due to heterogeniety of sand packing and high permeability of the material.

INTRODUCTION

The mathematical structure of the chemical transport model component describing the interaction of a chemical in, or on, the soil surface with surface runoff is extremely important. The mathematical structure and the parameter values assigned control the computed rate of removal of a chemical by shallow overland flow. Until recently, however, there have been very few experimental investigations of the processes involved. Recently, a few investigators have recognized that existing model structure is based on convenient assumptions rather than rigorous analyses verified by experimental data, and have conducted laboratory experiments on the exchange of chemicals present in the soil water with raindrop-disturbed overland flow (Ingram, 1979; Ingram and Woolhiser, 1980; Ahuja et al., 1981a; Snyder, 1981; Ahuja, 1982; Ahuja and Lehman, 1983). Ingram (Ingram, 1979; Ingram and Woolhiser, 1980) examined the removal of $CaSO_4$ solution from a saturated sand in a small laboratory flume with no infiltration. Ahuja et al. (1981a) and Ahuja (1982) measured the removal of P and Br from shallow prewetted soil boxes with nearly steady infiltration rates. Both groups of investigators used simulated rainfall to generate surface runoff and to provide a realistic disturbance at the surface. The data obtained from these experiments were used to estimate parameters and to test simple mixing zone models, and to estimate the depth of interaction of rainfall and runoff with the soil water.

Because infiltration velocities control not only the amount of surface runoff, but also the downward rate of removal of solute within the interaction zone, they should exert a significant effect on the chemical exchange process. This effect has been verified by Snyder (1981) and by Ahuja and Lehman (1983).

The objective of this paper is to describe an experimental apparatus designed to allow visualization of the mixing process near the soil-water interface with a controlled infiltration rate, and to present an analyses of the comparative effects of infiltration relative to slope, rainfall intensity, and kinetic energy on chemical transport into overland flow.

METHODS AND MATERIALS

Experimental Apparatus

The experimental apparatus, shown in Fig. 1, was constructed of clear 1.3-cm plexiglass to allow visualization of the loss of a dye tracer from the mixing zone. The nominal dimensions of the flume were: width 10 cm, length 200 cm, and depth 30 cm. Infiltration could be simulated and controlled by adjusting the elevation of a hose connected to a water-filled chamber at the bottom of the flume. Concentrations of dye tracer in the saturated porous medium were measured by sampling from five groups of sampling ports located along the length of the flume. In each group, the rubber septa sampling ports were located at 0.5-, 1.0-, 2.0-, 3.0-, 4.0-, and 5.0-cm depths into the porous medium. The soil layer was separated from the chamber at the bottom of the flume by a metal screen and nylon filter cloth. A hydraulic jack was placed under the flume so that it could be tilted.

Ottawa sand was chosen as the porous medium, because its light color allowed visualization of concentration gradients of Pontacyl Brilliant Pink-B dye, and its inert nature virtually eliminated dye adsorption.

Article was submitted for publication in January, 1985; reviewed and approved for publication by the Soil and Water Div. of ASAE in June, 1985.

The authors are: J. K. SNYDER, Project Engineer, Roy F. Weston, Inc., West Chester, PA; and D. A. WOOLHISER, Research Leader, USDA-ARS, Southwest Rangeland Watershed Research Center, Tucson, AZ.

Acknowledgments: These experiments were carried out at Colorado State University when the senior author was a Graduate Research Assistant and the junior author was Research Hydraulic Engineer, USDA-ARS, Fort Collins, CO. We thank Laj Ahuja for providing the numerical solutions for flow in a tilted slab, shown in Figs. 7 and 9, and D. McWhorter and John Brookman for providing laboratory facilities and helpful advice.

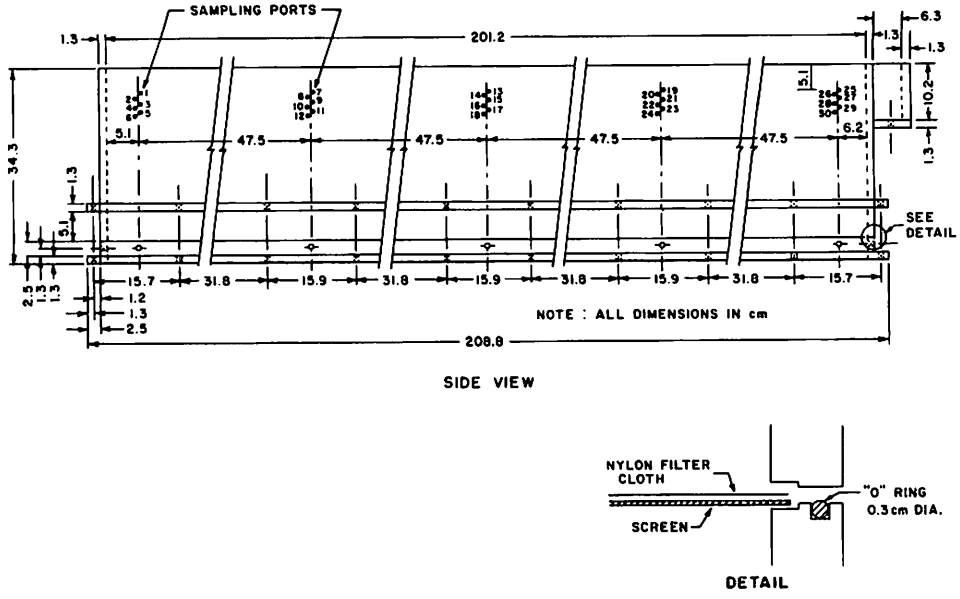

Fig. 1a—Side view of soil flume showing location and numbering of sampling points.

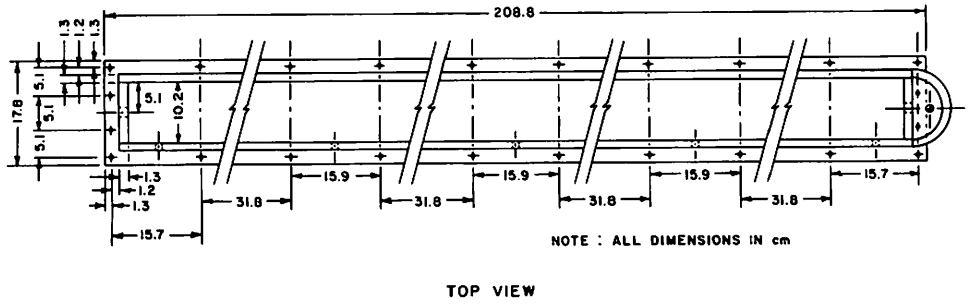

Fig. 1b—Top view of soil flume.

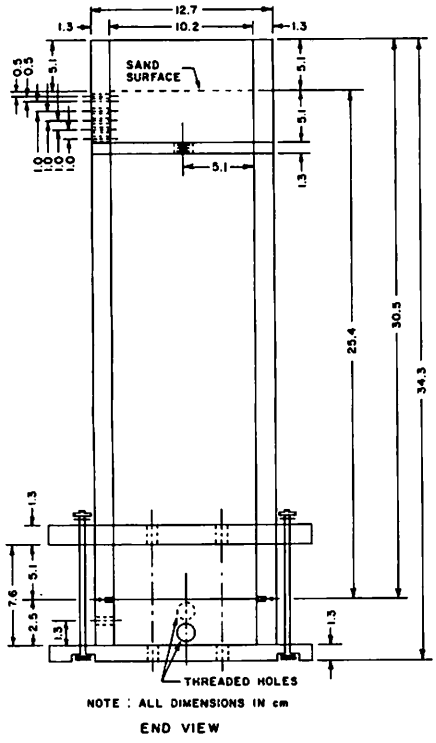

Fig. 1c—End view of soil flume.

Ottawa sand is quite uniform in particle size, having particle diameters between 0.2 mm and 0.6 mm. To ensure uniformity, the sand was placed in the flume in thin layers by pouring it from a 260 ML beaker with a long, sweeping motion along the length of the flume. The porosity of the Ottawa sand, using this placement technique, was 35%.

The saturated hydraulic conductivity of the Ottawa sand in the flume was 4.33 cm/min, considerably higher than would be encountered for field soils. The headloss through the sand, under normal infiltration rates, is quite small and, under conditions where the flume is tilted, the additional elevation head at the upper end of the flume will create a greater infiltration rate at the upper end of the flume than at the lower end. The sensitivity of the infiltration rate to the head differential between the surface of the sand and the bottom chamber was reduced by adding a layer of low hydraulic conductivity material beneath the Ottawa sand. We found that Mount St. Helen's ash, from Pullman, Washington, with a hydraulic conductivity of 4.0×10^{-3} cm/min, worked quite well for this purpose. To keep the fine ash particles from passing through the screen, and to keep the ash and Ottawa sand layers separate, thin layers of a fine silica sand were placed between the ash and Ottawa sand layers, and beneath the ash layer. The porous media characteristics are summarized in Table 1.

Chlorine-free water was used in the rainfall modules to prevent oxidation of the fluorescent dye tracer

TABLE 1. SUMMARY OF MEDIA CHARACTERISTICS.

Layer	Material	Hydraulic conductivity, cm/min	Particle density, g/cm^3	Porosity, ϕ,%	Depth of layer, cm
1	Ottawa sand	4.33	2.65	35	13.0
2	Silica flour	3.42×10^{-1}	2.65	40	1.5
3	Mt. St. Helen's ash	4.0×10^{-3}	2.53	62	11.1
4	Silica flour	3.42×10^{-1}	2.65	40	1.0

(Buchberger, 1979). Water was supplied to the rainfall modules from a Mariotte siphon, which allowed a constant pressure head to be applied to the inlet of the rainfall modules throughout the duration of the simulated rainstorm. A calibration curve of the rainfall rate versus head-loss relationship for the modules was determined so that an approximate rainfall rate could be set at the beginning of the experiment. To randomize the pattern of rainfall on the soil, the rainfall modules were oscillated by an electric motor. The rainfall rate could be adjusted by raising or lowering the Mariotte siphon supplying water to the rainfall modules. The kinetic energy delivered by the raindrops could be controlled by adjusting the height of the rainfall modules above the sand surface.

To determine the kinetic energy delivered by the raindrops, individual raindrops were collected and weighed to determine the mass of an average raindrop produced by the modules. Assuming a spherical shape for the raindrops, and knowing the height of fall, the kinetic energy of the raindrop upon impact with the soil could be calculated. Since various rainfall rates were used, and the duration of the simulated rainstorm was not exactly the same from one simulation to another, the total applied kinetic energy from raindrops for the entire storm was used as an independent variable.

Runoff from the flume was collected in a 15-cm diameter cylinder of PVC pipe, which was mounted vertically with an inlet at the bottom of the cylinder. A pressure transducer was attached to a separate connection at the bottom of the cylinder so that the volume of runoff collected in the cylinder at any time during the storm could be determined from the transducer's voltage reading. The volume versus voltage relationship for the cylinder was calibrated prior to the experiments. The total runoff collected at the end of the run was measured directly for three of the experimental runs to verify the calibration of the transducer.

The four hydrologic parameters, rainfall rate, height of fall, slope, and infiltration rate could be varied independently, and the rainfall rate and infiltration rate components were calibrated prior to the experimental simulations. A schematic diagram of the experimental apparatus is shown in Fig. 2.

EXPERIMENTAL PROCEDURES

To investigate the effects of the hydrological variables; slope, infiltration rate, and rainfall kinetic energy on chemical extraction and transport by overland flow, we wished to obtain samples of dye concentration in the surface runoff as a function of space and time, $C_s(x,t)$, and also samples of the dye concentration in the pore fluid as a function of horizontal distance, x, vertical distance, z, and time $C_p(x,z,t)$. With these data, we anticipated that we could compare spatially distributed models with the commonly used lumped models.

The combinations of experimental variables that were

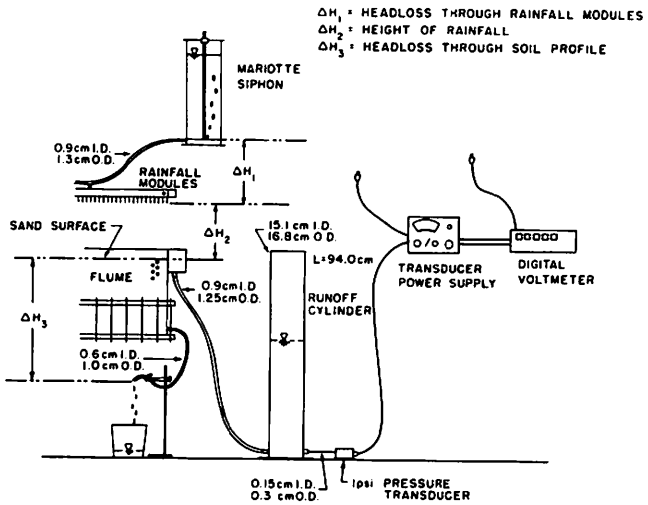

Fig. 2—Schematic diagram of the experimental apparatus.

investigated are summarized in Fig. 3. Three infiltration rates were investigated: 0.0, 0.434, and 0.731 cm/h. Two heights of rainfall, 46 cm and 76 cm, and four surface slopes, 0.0, 0.5, 1.0, and 3.0% were used. Time constraints prevented the investigation of all combinations of these variables, however. The initial concentration of dye for all experiments was 200 mg/L, and the duration of rainfall was approximately 30 min for all runs. The rainfall rates were adjusted so that the rate of rainfall excess (i.e., rainfall rate minus the infiltration rate) was nearly constant at approximately 4.3 cm/h.

The flume was initially leveled and saturated from the bottom upward to minimize the amount of air trapped in the sand. After the sand was completely saturated, a shallow depth of water was kept on the surface to prevent air from reentering the pore spaces. The top 6 cm of the soil profile was saturated with a 200 mg/L solution of Pontacyl Brilliant Pink-B dye by attaching a Mariotte syphon at the outlet of the flume and raising it to a level that allowed a uniform depth of about 1 cm of dye solution to cover the sand surface. Infiltration was then started and allowed to proceed until the top layer of sand was saturated uniformly. It was not necessary to saturate the entire profile with dye, because the depth of the sand layer that contributed dye to the overland flow was always less than 5 cm. At the start of the run, after the

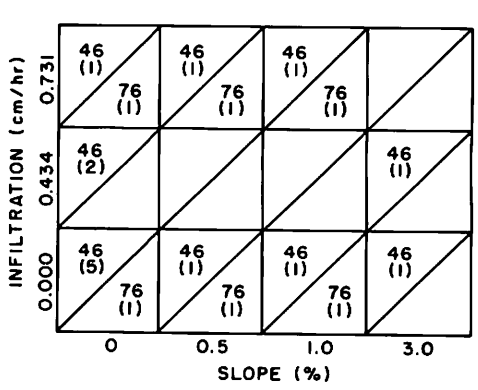

Fig. 3—Summary of experimental conditions.

top layer of sand had been saturated with the dye solution, the siphon was lowered, and the excess dye solution on the sand surface was allowed to drain back into the siphon. When the solution surface was lowered to coincide with the sand surface (i.e., the sand was completely saturated, with no water standing on the surface), the siphon was removed, and the runoff cylinder was attached to the outlet. The flume was then covered with a plastic sheet, the siphon supplying the water to the rainfall modules was set at the required elevation and, if the run involved infiltration, the elevation of the outlet base was set to create the desired rate. To start the run, the outlet hose was unclamped, the flume was tilted to the appropriate slope, and rain was applied by removing the plastic sheet.

Because the sand was saturated, surface runoff began almost immediately. The removal of the dye solution from the sand could be observed visually, and recorded photographically as the clear rainfall replaced the dye solution in the pore fluid. Dye concentrations in the overland flow and in the pore fluid were measured by removing 10 to 30 μL of water from the surface film or through the rubber septa sampling ports with a Hamilton No. 701-RN or No. 705-SN microsyringe. The sample from the microsyringe was then diluted to a known volume, and the dye concentration was determined by fluorometry. The microsyringe technique was tested in a column study and found to be capable of detecting the concentration gradients that we expected to observe in the mixing zone.

EXPERIMENTAL OBSERVATIONS

Twenty-one experimental runs were completed during the course of this investigation. A summary of the experimental conditions for each run is shown in Table 2.

Experiments with Zero Slope

For the 10 experiments with zero slope, there was no apparent lateral flow within the sand. Although there was a greater depth of overland flow at the upper boundary than at the lower boundary, this difference caused no noticeable variation in the depth to which dye was removed.

Because of the time required to obtain samples, and the large sampling variability, we could not obtain a sufficiently large number of samples to detect differences in concentration with distance in the downstream direction either within the surface runoff or in the porous medium. The large sampling variability also masked any differences between runs due to the rainfall excess rates. Consequently, all observations for all runs with zero slope and zero infiltration rate were lumped together. Regression techniques were used to estimate the relationship between concentration and time for surface runoff and the pore fluid at the 0.5 cm and 1 cm depths. Both linear and exponential relationships were tried for infiltration rates of 0, 0.434, and 0.731 cm/h, and the best fit curves are shown with the data in Fig. 4. Dye concentrations in surface runoff and pore fluid at five-minute intervals were obtained from the curves of Figure 4, and are plotted in Figs. 5 and 6.

Although there was a great deal of scatter in the data at the 0.5 cm and 1 cm depths, it appears that some dye was removed to a depth between 1 and 2 cm. For the runs with no infiltration (Fig. 5), the concentration profiles are convex upward for the first 25 min. The concentration increases rapidly with depth below the surface, asymptomatically approaching the initial concentration of 200 mg/L. These concentration profiles are similar to those measured by Ahuja and Lehman (1983) for impervious base soil boxes. There is some indication that at t = 30 min, the concentration depth curve is beginning to assume an "S" shape. For the runs with infiltration (runs 6 and 7, shown in Fig. 6), the concentration profile exhibits an approximate "S" shape at all times, reflecting the combined effect of convective dispersion induced by infiltration and the mixing and removal induced by the raindrops.

TABLE 2. SUMMARY OF EXPERIMENTAL RESULTS.

Run no.	Slope, s, %	Infiltration rate, i, cm/h	Height of rainfall, cm	Length of run, min	Total runoff volume, L	Rainfall excess rate, R, cm/h	Total kinetic energy delivered, E, J	Effective mixing zone depth, ϵ', cm	Average depth of dye removal ϵ'', cm	Mass of dye in runoff, mg
1	0	0	46	26	5.872	6.453	24.1	0.930	0.8	131.9
2	0	0	46	32	6.177	5.515	25.4	0.734	0.428	106.5
3	0	0	46	38	5.667	4.261	23.3	0.664	0.3	89.8
4	0	0	46	30	5.435	5.176	22.3	0.456	— —	65.7
5	0	0	46	30	5.495	5.233	22.6	0.582	0.5	78.7
6	0	0.434	46	30	4.499	4.285	20.3	0.427	0.38	62.4
7	0	0.434	46	30	5.635	5.367	25.0	0.474	0.507	69.1
8	3	0.434	46	30	4.755	4.529	21.4	1.787	2.270	262.6
9	3	0	46	30	5.524	5.261	22.7	2.142	1.270	314.6
10	0	0.731	46	30	2.994	2.851	15.4	0.388	0.300	56.4
11	1	0	46	30	4.68*	4.457	19.2	1.448	0.681	200.1
12	1	0.731	46	30	4.69*	4.467	22.4	0.901	0.336	127.1
13	0.5	0	46	30	4.552	4.335	18.7	1.410	0.865	154.4
14	0.5	0.731	46	31	5.066	4.669	24.1	0.767	0.079	106.0
15	1	0	76	30	4.69*	4.467	30.0	1.451	0.902	200.5
16	1	0.731	76	30	4.505	4.290	33.7	0.721	0.265	98.1
17	0	0	76	30	3.981	3.791	25.4	1.132	2.35	92.8
18	0	0.731	76	30	4.23	4.029	31.9	0.303	0.456	43.9
19	0.5	0	76	30	2.885	2.746	18.4	1.831	1.123	158.8
20	0.5	0.731	76	30	3.522	3.354	27.4	0.754	0.622	195.1
21	1	0	35†	30	4.279	4.075	— —	1.407	0.807	195.1

*Measured directly.
†The surface of the sand was covered with nylon filter cloth and screen to minimize the kinetic energy for this run.

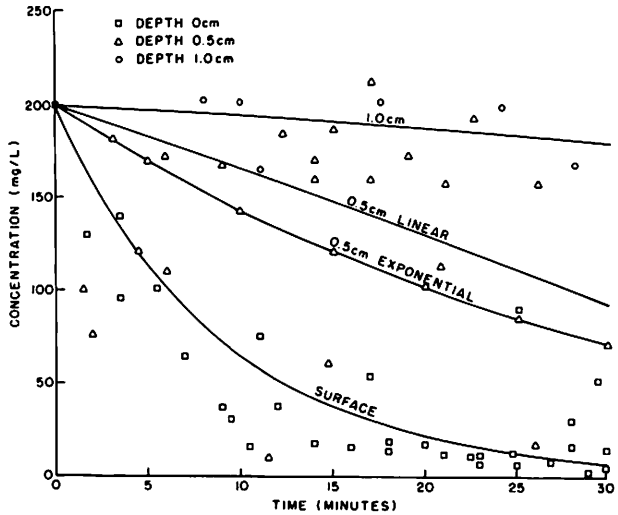

Fig. 4a—Concentration vs. time (infiltration = 0).

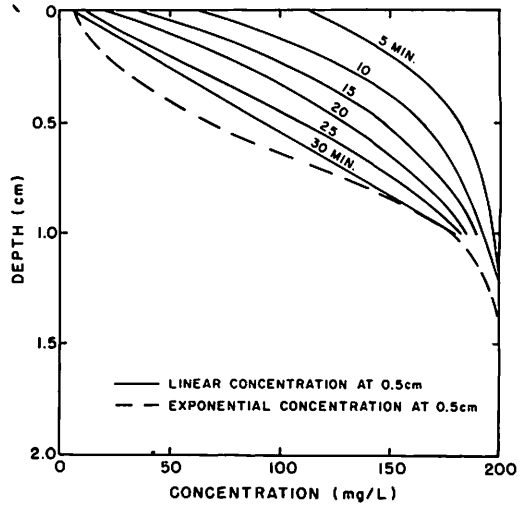

Fig. 5—Average concentration profiles (slope = 0; infiltration = 0).

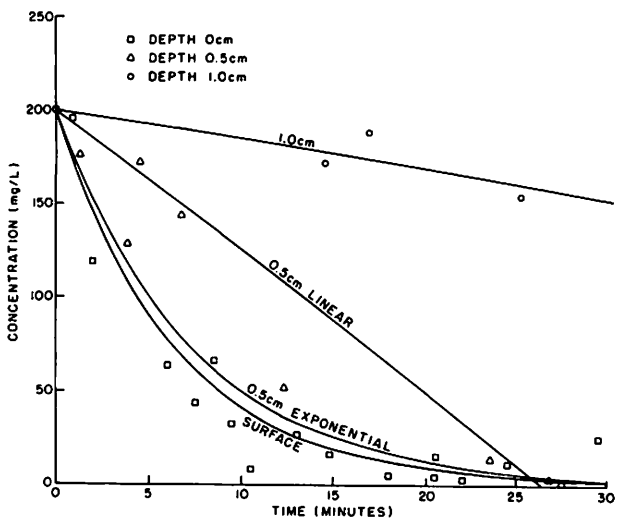

Fig. 4b—Concentration vs. time (infiltration = 0.434 cm/h).

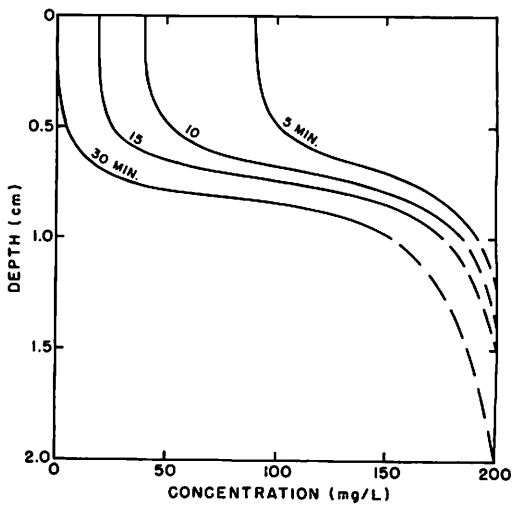

Fig. 6—Average concentration profile (slope = 0; infiltration = 0.434 cm/h).

The average concentration deficit at the end of the runs (30 min) was integrated with respect to depth to estimate the average mass of dye removed with and without infiltration. For the zero infiltration cases, the mass of dye removed for the average profile, assuming linear concentration-time functions at 0.5 and 1 cm depths, was 77.6 mg, compared with the average measured mass of dye of 94.2 mg. With infiltration of 0.434 cm/h, the calculated amount of dye removed, in addition to calculated convective displacement, was 42 mg, as compared with the average of the measured removals of 66 mg. Correcting for convective displacement by using a plug flow assumption should result in an underestimate of the dye removal, so it appears that the 30-minute concentration profiles in Fig. 5 are approximately correct. If the exponential concentration-time curve at 0.5 cm depth is used to construct the profile (the dashed line in Fig. 5), the calculated dye removal is 88 mg. Thus, it appears that the "s" shaped curve at 30 min is the most appropriate.

Insufficient data were taken at the higher infiltration rate (0.731 cm/h) to prepare concentration versus depth curves. However, the concentration in the surface runoff decreased at a faster rate than for 0.434 cm/hr, and an exponential function provided a reasonably good fit to the data.

Experiments with Slopes from 0.5 to 3%

Because of the relatively high hydraulic conductivity of the porous medium used in this study, it was anticipated that some lateral flow, or "interflow," would occur when the flume was tilted, with or without infiltration. In a theoretical analyses of saturated flow through a sloping layered soil, Ahuja et al. (1981b) found that, for impermeable subsoils, the water enters and leaves the soil near the upper and lower corners. However, for the case where the slope length is 10 times the soil thickness, the stream lines are parallel to the slope for most of the slope length. The ratio of the length of flume to the total depth is somewhat less for our apparatus, but flow paths calculated from the mathematical expressions developed by Ahuja, et al. (1981b) led to the same conclusions. The soil flume system was represented as a two-layer system, with the ratio of the hydraulic conductivity of the subsoil, K_2, to that of the topsoil, K_1, of 9.24×10^{-4}. Flow lines calculated for this conductivity ratio with the geometry of our apparatus, a slope of 3% and zero infiltration, are shown in Fig. 7. Experimental run 9 was performed

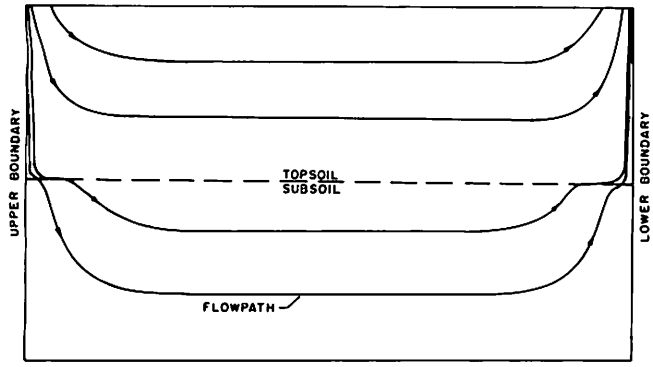

Fig. 7—Predicted flow paths through a two-layer porous media system having a 3% slope and no infiltration.

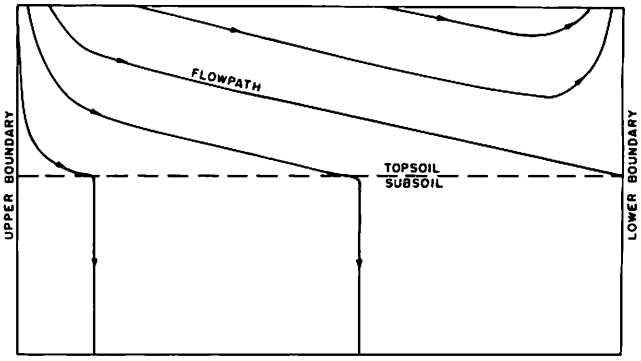

Fig. 9—Predicted flow paths through a two-layer porous media system having a 3% slope and a positive infiltration rate.

under these conditions; however, the flow lines that could be inferred by the visible dye profile, during and after the run, were quite different, with water entering and leaving the surface at two positions along the slope. The zones of infiltration and exfiltration were clearly visible during the experiment, with the infiltration zones bcoming progressively lighter as the dye was removed, while the exfiltration zones remained a brilliant pink, and the surface runoff became more pink as it passed over an exfiltration zone. The visible dye profile at the end of run 9, and the inferred flow paths, are shown in Fig. 8.

The theoretical streamlines for the case of constant infiltration of 0.434 cm/h through the lower boundary are shown in Fig. 9. Except for a small area near the lower corner, there is a net downward flux at the surface. Experimental run 8 was performed under these conditions. The visible dye removal patterns for the run, as shown in Fig. 10, appear to be in close agreement with the theoretical pattern shown in Fig. 9, but this is the only case when close agreement could be found. The very complex dye removal patterns for runs 15 and 16, shown in Fig. 11, demonstrate this unexpected phenomenon.

The capillary tubes of the rainfall simulator were operating uniformly, and were eliminated as a possible cause of the unusual flow paths. To investigate the possibility that an interaction between raindrop inpact and overland flow depths contributed to the observed patterns, run 21 was performed under conditions such that the kinetic energy of the raindrops was substantially reduced. This was achieved by lowering the rainfall modules to a height of 35 cm, then covering the sand with a layer of nylon filter cloth and a layer of metal screen. The flume was tilted to a 1% slope so significant interflow should occur. The wave-like patterns of infiltration and exfiltration were still observed. The only apparent explanation is that the patterns are caused by variations in hydraulic conductivity due to heterogeneous packing of the sand. The fact that the dye removal

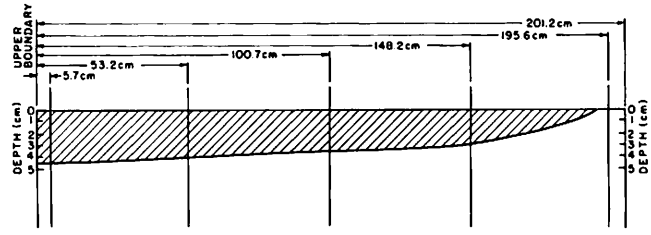

Fig. 10—Dye removal observed after Run No. 8.

pattern for the first run with non-zero slope (run no. 8) was consistent with the theoretical pattern of flow, while the patterns for the subsequent runs were not, suggests that some of the variations in hydraulic conductivity were flow-induced.

Average concentration versus depth profiles for the runs with slopes greater than zero have little meaning, because the observed flow differs so much from the theoretical flow paths. However, an effective mixing zone depth ϵ' can be calculated from the expression developed by Ingram (1979)

$$\epsilon' = \frac{\text{Total Outflow of Mass}}{(C_{m1} - C_{m2})\, A\phi} \quad \ldots\ldots\ldots\ldots\ldots\ldots [1]$$

where C_{m1} = the concentration of solute in the mixing zone at the beginning of the run (ML^{-3})

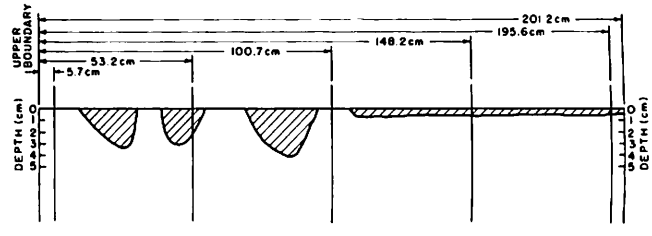

Fig. 11a—Dye removal observed after Run No. 15.

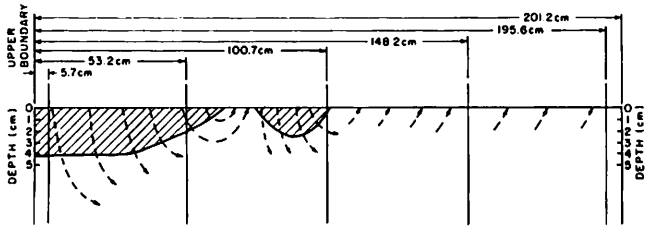

Fig. 8—Area of visible dye removal observed after Run No. 9.

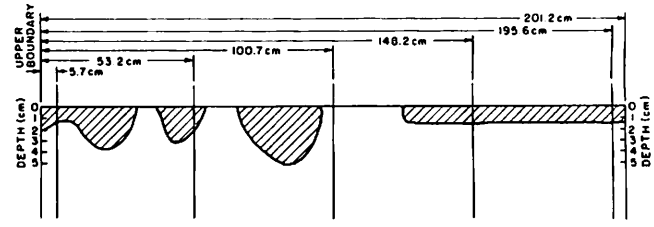

Fig. 11b—Dye removal observed after Run No. 16.

C_{m2} = the concentration of solute in the mixing zone at the end of the run (ML^{-3})
A = the horizontal area of the flume (L^2)
ϕ = the porosity of the saturated sand (0.35).

In this approach, it is assumed that the dye is removed uniformly to a depth ε', and that the concentration in the mixing zone is a function only of time. Equation [1] will greatly underestimate ε' due to chemical removed from the mixing zone by infiltration and the effects of interflow.

The total mass of dye transported from the flume was calculated from the measured concentrations and volumes at the end of each run. In calculating values of ε', average measured values of C_m at 0.5 cm depth were used for C_{m1} and C_{m2}. An underestimation of the mixing zone depth index, ε', results when the concentration of solute in the mixing zone at 0.5 cm depth is less than the average concentration of solute in the mixing zone. In many cases, the mixing zone was shallow, and measurement of the vertical concentration gradient was not possible. For all of the runs, except run 4, the average depth of visible dye removal ε'', was measured and compared with the calculated mixing zone depth index, ε'.

The downward flux of pore fluid caused by infiltration causes the visible depth of dye removal to increase, even though the actual mixing zone depth will remain nearly the same. In order to compare the values of ε'' between the simulations, with and without infiltration, the depth due to infiltration velocity was subtracted from the observed depth in those runs where infiltration was present.

The displacement due to infiltration is:

$$d = \frac{i\,t}{\phi} \quad \ldots\ldots\ldots\ldots\ldots\ldots\ldots\ldots\ldots\ldots [2]$$

where i is the infiltration rate (cm/hr), t is the duration of the run (hr), and ϕ is the porosity of the medium.

The mass of dye removed by runoff, the effective mixing depth, ε' calculated using equation [1], and the average depth of visual dye removal, ε'', corrected by the infiltration displacement, given by equation [2] are shown in Table 2.

Regression Analyses

The relationships between the effective mixing depths ε' and ε'', and their dependence upon the experimental variables, slope, infiltration rate, and rainfall rate were explored by regression analyses. The effective mixing depth ε' was related to the experimental variables by the following equation:

$$\varepsilon' = 1.72 + 0.46\ s - 0.71i - 0.18\ R \quad (r^2 = 0.86) \ldots [3]$$

when s is the soil surface slope (%), and R is the rainfall rate. The effect of kinetic energy was too small to be significant.

The negative coefficient on the infiltration rate can be explained by the fact that infiltration removes some of the dye before it can be transported into the overland flow by raindrop induced mixing. This reduces the total mass transported in the overland flow, and from equation [1], it can be seen that this reduces the value of the effective mixing zone depth index, ε'.

The negative coefficient on the rainfall term can be explained in terms of the protective effect of greater depths of overland flow associated with greater rainfall rates. Less mixing, or transfer of solute from the mixing zone into the overland flow, would be expected to occur when more of the raindrop energy is dissipated in the form of splash, since less energy is transferred into the mixing zone. A correlation between rainfall rate and infiltration rate is a result of the experimental constraint of maintaining a constant rainfall excess rate, and also contributes to the negative coefficient on the rainfall rate term in equation [3].

Although the rainfall excess rate for all of the experimental runs was nearly constant, this does not mean that the flow depth profiles were the same for a given slope for different infiltration rates. It has been shown in laboratory studies (c.f. Li, 1972) that, when the flow Reynolds number is in the laminar range, the Darcy-Weisbach friction factor f can be expressed in the form:

$$f = \frac{K_0 + g(R)}{R_e} \quad \ldots\ldots\ldots\ldots\ldots\ldots\ldots\ldots\ldots\ldots [4]$$

where R_e is the flow Reynolds number, K_0 is a constant which depends upon the surface roughness, and g(R) indicates some increasing function of rainfall rate. Thus, with a constant flow Reynolds number (constant discharge per unit width), the friction will increase with the rainfall rate, resulting in greater flow depths and decreased average velocities.

The visually observed mixing zone depth ε'' and the computed depth ε' were linearly related ($r^2 = 0.42$). However, ε' was greater than ε'', possibly due to the threshold of visual detection of dye in the sand medium, which results in an underestimation of ε''.

Because the effective mixing depth ε' involves an assumption of uniformity of concentration in the downslope direction, and is calculated from M, the total mass of dye removed, we also investigated simple linear relationships between M and the experimental variables. The regression equation is:

$$M = 126.1 + 70.4\ s - 73.1\ i - 0.41\ E - 2.09\ R \quad (r^2 = 0.93) \ldots\ldots\ldots\ldots [5]$$

where E is the kinetic energy of the simulated storm, in Joules.

Clearly, the slope and infiltration terms are very important, and their signs are as anticipated because greater slopes lead to significant interflow. We had anticipated that M would be positively related to kinetic energy, as observed by Ingram (1979). However, it appears that the positive correlation between E and R, the positive correlation between R and i, and experimental errors combine to give a coefficient with sign contrary to what would be predicted from physical considerations.

DISCUSSION AND CONCLUSIONS

The experimental apparatus, designed to visualize the mixing process between surface runoff and tracer dyes in a porous medium, was successful in many respects. The mixing process at the surface was easily observed

through the plexiglass walls of the flume, and the removal of dye left a clearly visible "washed out" area near the surface. Infiltration could be closely controlled by changing the head in the lower chamber. The microsyringe technique, to obtain samples of the dye concentration in the pore fluid, was also satisfactory. The variability of the dye concentration over short distances and times was much greater than anticipated, possibly reflecting the fact that the location of raindrops impacting the surface was not random. Although the capillary tubes were oscillated in a circular or elliptical path, and the drops appeared randomly along these paths, they did not cover the surface of the flow uniformly.

When the flume was level, so that interflow was negligible, the dye concentration profiles in the sand without infiltration were convex upward for times less than 25 min, with concentration increasing rapidly with depth below the surface, and then asymptotically approaching the original uniform concentration at approximately 1.5 cm depth. At 30 min, the profiles assumed an "S" shape. The dye profiles, for the runs with infiltration, had an approximate "S" shape at all times, reflecting the combined effects of convective dispersion induced by infiltration and the mixing effect of raindrops. It would appear from these profiles that a convective dispersion model, with the dispersion coefficient increasing near the surface, could be used to describe the detailed movement of chemicals within the mixing zone (Ahuja and Lehman, 1983). The commonly used complete mixing model, in which the solute concentration in a mixing zone of depth ε is assumed to be equal to the concentration in overland flow, apparently is not a bad approximation to the inferred solute concentration profiles for high infiltration rates shown in Fig. 6. However, with low infiltration rates, or with no infiltration, it appears that an incomplete mixing model would provide a better approximation to the inferred solute concentration profile (Ahuja and Lehman, 1983).

Unexpected complex patterns of infiltration and exfiltration were observed at the surface of the porous media when the flume was tilted. These patterns were apparently caused by variations in the hydraulic conductivity of the sand due to nonuniformities of packing or flow induced variations in hydraulic conductivity. This phenomenon may be important in the field. It certainly seems likely that, if these complex flow patterns were observed under laboratory conditions where every effort was made to ensure uniformity, then this phenomenon would most likely also occur in the field. Thus, except for infiltration at the upper end and exfiltration near the lower boundary, it is highly unlikely that the flow lines for interflow through a sloping topsoil overlying a less permeable subsoil will approximately parallel the slope. Rather, there may be several zones of infiltration and exfiltration along the slope, and chemicals found in surface runoff at midslope may have been contributed by interflow as well as by surface exchange processes.

The mass of dye removed in overland flow was positively related to slope of the flume and negatively related to the infiltration rate, the rainfall rate and the kinetic energy of the rainfall. The magnitude of the regression coefficients suggests that for these experiments, slope and infiltration rate are of primary importance in chemical transport, followed by rainfall rate and kinetic energy. The positive effect of slope is probably due to the significant interflow when the flume is tilted. Infiltration reduces the amount of dye transported by overland flow, because it is removed from the mixing zone. The negative effect of rainfall rate can be explained by the "cushioning" effect of greater depths of surface runoff and its experimental correlation with infiltration. The negative effect of kinetic energy is contrary to what we would expect from physical reasoning, and may be due to the correlation between rainfall rate and kinetic energy, as well as experimental errors.

It would be instructive to conduct experiments similar to those conducted in this study using a porous medium with a conductivity in the range that might be encountered in a natural field situation. The fine silica flour, used to separate the Mount Saint Helen's ash layer from the other layers, has a relatively low hydraulic conductivity of approximately 0.725 cm/min, and has the additional advantage of being fairly inert to the fluorescent dye tracer, is readily and economically available, and has a light color which allows for good visualization of concentration gradients of dye tracers in this medium. This would be an excellent medium to use in tests similar to those conducted in this study.

References

1. Ahuja, L. R., A. N. Sharpley, M. Yamamoto, and R. G. Menzel. 1981a. The depth of rainfall-runoff-soil interaction as determined by ^{32}P. Water Resources Research 17(4):969-974.
2. Ahuja, L. R., J. D. Ross, and O. R. Lehman. 1981b. A theoretical analysis of interflow of water through surface soil horizons with implications for movement of chemicals in field runoff. Water Resources Research, 17(1):67-72.
3. Ahuja, L. R. 1982. Release of a soluble chemical from soil to runoff. TRANSACTIONS of the ASAE 25:948-953, 960.
4. Ahuja, L. R., and O. R. Lehman. 1983. The extent and nature of rainfall-soil interaction in the release of soluble chemicals to runoff. J. Environ. Qual. 12:34-40.
5. Buchberger, S. G. 1979. The transport of soluble nonpoint source pollutants during the rising hydrograph. M.S. Thesis, Colorado State University, Fort Collins.
6. Ingram, J. J. 1979. Chemical transfer from a saturated soil into overland flow. M.S. Thesis, Colorado State University, Fort Collins.
7. Ingram, J. J., and D. A. Woolhiser. 1980. Chemical transfer into overland flow. Proc. Symposium on Watershed Management '80, ASCE, Boise, ID, pp. 40-53.
8. Li, Ru-Ming. 1972. Sheet flow under simulated rainfall, M.S. Thesis, Dept. of Civil Engineering, Colorado State University, Fort Collins.
9. Snyder, J. K. 1981. Experimental investigation of rainfall, runoff, and soil water interaction. M.S. Thesis, Dept. of Civil Engineering, Colorado State University, Fort Collins.